High-Altitude Flight Control of a Micro Air Vehicle Using Only Two Sensors

A. Kahn and D. Edwards
Tactical Electronic Warfare Division

Purpose: The Vehicle Research Section of the Naval Research Laboratory's Tactical Electronic Warfare Division designed an experiment to evaluate whether a small, low-cost, expendable air vehicle could be released from high altitude and fly autonomously to a preprogrammed location on the ground. Such a technology could emplace ground/ocean sensors, insert last-mile network connectivity nodes, or deliver critical medical drugs to difficult-to-access areas.

Design Considerations: A key element of the experiment was to keep the overall manufacturing cost of the vehicle to a minimum. Two unique design elements help achieve this goal. First, vehicle manufacturing and assembly are simplified by the dual use of the autopilot electronics circuit card also as the air vehicle's structure and wing. The highly automated PC board fabrication process simultaneously produces the major airframe components. Second, hardware cost and complexity are kept to a minimum by utilizing only two sensors, a rate gyroscope and GPS receiver, for navigation and flight control of the vehicle.

The Vehicle Design: CICADA (Close-In Covert Autonomous Disposable Aircraft) is the result of this design effort, shown in Fig. 1. The air vehicle is a glider, with simple flight controls on the wing to control pitch and roll. The CICADA design has a wingspan of 36 cm, length of 20 cm, and mass of 226 g. The vehicle electronics are powered by small cellphone-like lithium batteries and an internal heater keeps these battery cells warm in the extreme cold present at altitudes in excess of 9000 m. All the electronics are also encased in polyurethane foam to provide thermal insulation and to protect against condensation.

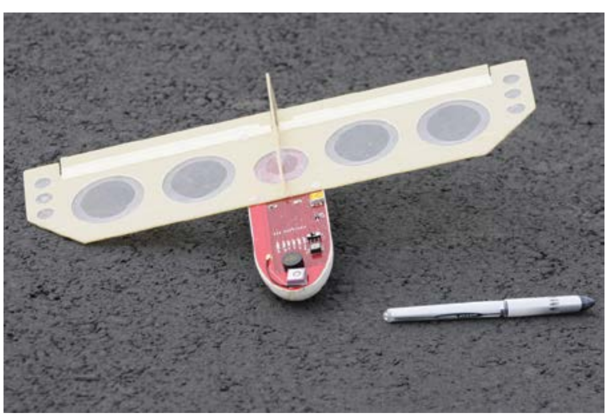

FIGURE 1
CICADA air vehicle.

Flight Control: Navigation and control for the CICADA uses only two simple sensors: a roll-rate gyroscope and a GPS receiver. The navigation system estimates the roll attitude and vertical descent rate of the vehicle. Roll attitude is estimated by using the rate of change of the ground track from the GPS and the roll-rate signal from the gyroscope. Vertical descent rate is estimated using GPS altitude measurement along with an a priori measurement of the vehicle's lift-to-drag ratio. These two estimated states provide the necessary measurements to control the roll and pitch attitude of the vehicle using traditional linear proportional-integral-derivative controllers.

Guidance of the CICADA is broken into two flight modes. First, the vehicle flies in a straight line toward the preprogrammed landing location. Once the vehicle is sufficiently close to the target location, the guidance system then directs the vehicle to orbit around the landing location until impact with the ground.

Results: Flight tests were performed at the Army's Yuma Proving Ground by mounting two CICADA air vehicles to the wings of a mother-ship unmanned air vehicle. The assembly was then flown to high altitude using a weather balloon, as seen in Fig. 2. At high altitude, the mother-ship was released from the balloon and flew about halfway toward the desired target location. Then, the CICADA vehicles were released from the mother-ship for final ingress to the target landing location. The flight path from one CICADA is shown in Fig. 3, illustrating the precision control of this small air vehicle. Fourteen high-altitude flights showed that the CICADA could repeatedly land within 5 m of the preprogrammed location. These results proved the robustness of this minimal, yet capable vehicle and control system.

Conclusions: This experiment demonstrated that a small, low-cost, expendable vehicle can be launched from high altitudes and precisely land at a preprogrammed location. This work provides the ability to emplace such items as ground/ocean sensors, deliver critical medical drugs, or insert last-mile network connectivity nodes into difficult-to-access locations. The unique design of the air vehicle allows for highly automated manufacturing methods to be used, thereby keeping per-unit costs low, without sacrificing the precision needed by tomorrow's Navy.

FIGURE 2
High-altitude weather balloon lifting mother-ship UAV with two CICADA vehicles attached.

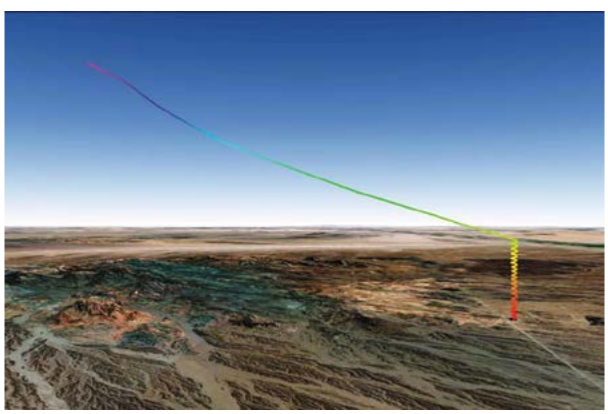

FIGURE 3
Flight path of the CICADA vehicle.

References

[1] A. Kahn and D. Edwards, "Navigation, Guidance and Control for the CICADA Expendable Micro Air Vehicle," AIAA Guidance, Navigation, and Control Conference, Aug. 2012, Minneapolis, MN, doi:10.2514/6.2012-4536.

[2] D. Edwards and A. Kahn, "Design Evolution of a High Packing Density Micro Air Vehicle for Local-Area Seeding," AIAA Atmospheric Flight Mechanics Conference, Aug. 2012, Minneapolis, MN, doi:10.2514/6.2012-4735.

♦

The Navy Global Environmental Model

T. Hogan,[1] M. Peng,[1] N. Baker,[1] C. Reynolds,[1] B. Ruston,[1] M. Liu,[1] J. Ridout,[1] S. Eckermann,[2] J. Moskaitis,[1] T. Whitcomb,[1] K. Viner,[1] J. McLay,[1] P. Pauley,[1] L. Xu,[1] R. Langland,[1] M. Flatau,[1] J. McCormack,[2] and S. Chang[1]
[1] *Marine Meteorology Division*
[2] *Space Science Division*

A New Global Model: The Navy Global Environmental Model (NAVGEM) is the U.S. Navy's new high-resolution global weather prediction system, replacing the existing Navy Operational Global Atmospheric Prediction System (NOGAPS), which was introduced in 1982. Development of NAVGEM was sponsored by the Office of Naval Research (ONR) and OPNAV N2/N6E (Oceanographer of the Navy). NAVGEM represents a significant NRL milestone in numerical weather prediction (NWP) system development by introducing a semi-Lagrangian/semi-implicit (SL/SI) dynamical core together with advanced moisture and ozone physical parameterization schemes. The new SL/SI dynamic core allows for much higher model resolutions without the need for small time steps. This capability has permitted NAVGEM's initial operational transition to have both higher horizontal and higher vertical resolutions than NOGAPS (50 vertical levels in place of NOGAPS's 42 levels and an increase of horizontal resolution from 42 km to 37 km); to include cloud liquid water, cloud ice water, and ozone as fully predicted constituents; to contain new moisture, solar radiation, and longwave radiation parameterizations; to contain significant upgrades to the data assimilation component; and to complete the 180 h forecast in the allotted operation window.

NAVGEM Advancements: Critical to NAVGEM's success is the new SL/SI dynamical core. The SL method is to find the trajectory of the fluid motion that starts at the previous time step and ends up at the NAVGEM grid point location.[1] The SL integration removes the Courant-Friedrichs-Lewy (CFL) limitation of NOGAPS for conventional fixed point integration of the dynamical equations; however, high-speed gravity waves associated with high-frequency fluctuations in the wind divergence remain. This is mitigated by incorporating an SI method into the SL integration, where the terms responsible for the gravity waves are identified and treated in an implicit manner, thereby slowing down the fastest gravity waves. The combined SL/SI schemes have enabled NAVGEM to run with a time step that is three times faster than NOGAPS. With the addition of cloud liquid water and cloud ice water advection, NRL has developed a new two-species microphysics cloud water parameterization based on the work of Zhao.[2] Convective clouds are allowed to evaporate at a finite rate that varies with cloud cover, providing for a more realistic representation of convective processes. This feature is enhanced by detraining cloud condensate between the lifting condensation level and the level of free convection in the NAVGEM modified versions of the Simplified Arakawa-Schubert and National Centers for Environmental Prediction (NCEP) Global Forecast System (GFS) shallow convection schemes.

Another significant improvement in NAVGEM is the addition of the Rapid Radiative Transfer Model for General Circulation Models (RRTMG) parameterizations for solar and longwave radiation, developed by Atmospheric and Environmental Research (AER, Lexington, MA).[3] RRTMG includes significantly more radiation frequency bands in the solar and longwave spectra than the previous NOGAPS radiation parameterizations and incorporates additional molecular absorbers and emitters. A unique feature of the RRTMG is the use of a Monte Carlo technique to compute the subgrid cloud variability and the vertical cloud overlap.

Satellite radiance observations typically account for more than 65% of the total assimilated observations in NAVGEM. The data assimilation component that brings these observations into NAVGEM is the NRL Atmospheric Variational Data Assimilation System – Accelerated Representer (NAVDAS-AR), which has been operational in NOGAPS since 2009.[4] The NOGAPS radiance bias correction method has been replaced in NAVGEM with a variational bias correction approach, which estimates the bias predictors simultaneously with the atmospheric analysis during each data assimilation cycle.[5] This way, the bias corrections are constrained by other observations, the NWP model, and the analysis procedure itself.

Accuracy and Forecast Skill: Verification of NAVGEM's accuracy shows significant improvements over NOGAPS. Figures 4 and 5 show the northern hemisphere 1000 hPa geopotential height anomaly correlations (AC) for summer 2012 and fall/winter 2012/2013, respectively. The AC, a fundamental metric used by all major NWP centers, is the normalized correlation of the forecast and analysis differences with climatology, with 1.0 being a perfect forecast. The NAVGEM 120 h near-surface forecasts show a 6 h improvement over the NOGAPS forecasts for this same parameter. Tropical cyclone (TC) track forecasts are of vital importance to the safety of U.S. Navy ships, aircraft, and personnel. Figure 6 shows the TC track error comparison in nautical miles (nmi) for summer/fall 2012. The NAVGEM 120 h TC track error is 30 nmi less than that in NOGAPS, approximately a 12 h improvement. Synoptic evaluations of daily weather maps show reduced

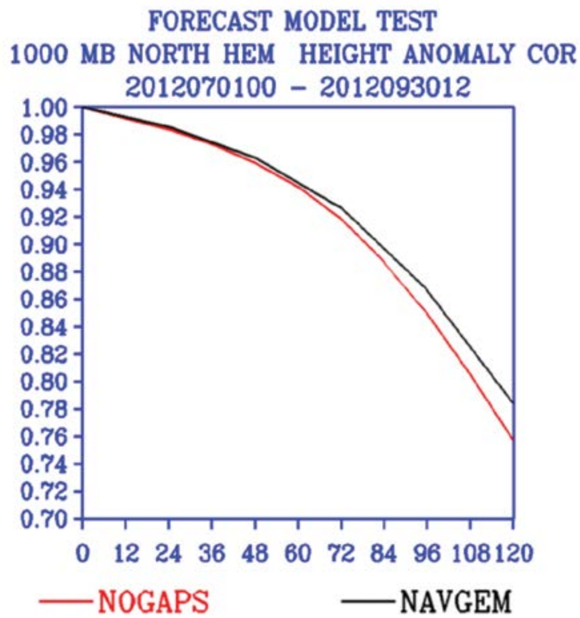

FIGURE 4
The 1000 hPa height anomaly correlations scores for NOGAPS and NAVGEM for the forecast period of July 1, 2012, to September 30, 2012.

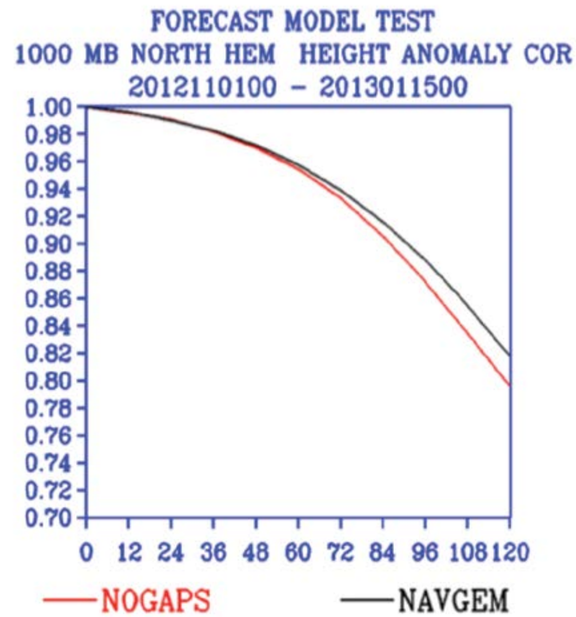

FIGURE 5
The 1000 hPa height anomaly correlations scores for NOGAPS and NAVGEM for the forecast period of November 1, 2012, to January 15, 2013.

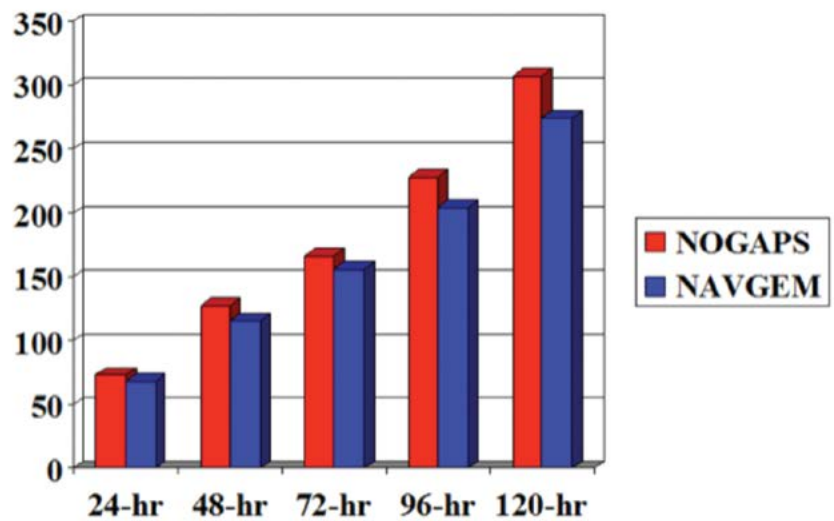

FIGURE 6
The tropical cyclone track errors in nautical miles for NOGAPS and NAVGEM for the period of July 1, 2012, to October 31, 2012. At 120 h there were 132 tropical storms that verified.

surface pressure errors with NAVGEM, particularly for maritime lows that impact the safety of ships at sea. In addition, the mid-level troughs associated with frontal systems were more realistic (deeper and faster moving) in NAVGEM than in NOGAPS.

An official operational test (OPTEST) of NAVGEM versus NOGAPS was conducted by Fleet Numerical Meteorology and Oceanography Center (FNMOC) for the period of November 6, 2012, to December 18, 2012, with a statistical evaluation based on FNMOC's standard global scorecard. This scorecard evaluates the comparative skill of the models based on AC, mean and root mean square errors of 16 different fields and observation types, including TC tracks, 10 m winds at buoy sites, 1000 hPa and 500 hPa AC, and winds and temperatures at radiosonde locations, assigning a weighted positive score to the model with statistically significant better forecasts. Improvements in all categories would yield a skill score of +24. NAVGEM scored a +14, the highest score ever obtained for a global model transition at FNMOC. Historically, global model improvements resulted in a skill improvement of +2. NRL will continue to upgrade NAVGEM with planned transitions to higher vertical and horizontal resolutions, a more computationally efficient dynamical core, further improvements to the data assimilation system, more advanced physical parameterizations, and the assimilation of data from recently launched satellite sensors.

[Sponsored by SPAWAR PMW-120]

References

[1] H. Ritchie, "Application of the Semi-Lagrangian Method to a Multilevel Spectral Primitive-Equations Model," *Q. J. R. Meteorol. Soc.* **117**, 91–106 (1991).

[2] Q.Y. Zhao and F.H. Carr, "A Prognostic Cloud Scheme for Operational NWP Models," *Mon. Wea. Rev.* **125**, 1931–1953 (1997).

[3] R. Pincus, H.W. Barker, and J.-J. Morcrette, "A Fast, Flexible, Approximate Technique for Computing Radiative Transfer in Inhomogeneous Clouds," *J. Geophys. Res.* **108**(D13), 4376 (2003); doi:10.1029/2002JD003322.

[4] B.S. Chua, L. Xu, T. Rosmond, and E.D. Zaron, "Preconditioning Representer-based Variational Data Assimilation Systems: Application to NAVDAS-AR," in *Data Assimilation for Atmospheric, Oceanic and Hydrologic Applications*, eds. S.K. Park and L. Xu, pp. 307–320 (Springer-Verlag, 2009).

[5] D.P. Dee, "Variational Bias Correction of Radiance Data in the ECMWF System," in Proceedings of the ECMWF Workshop on Assimilation of High Spectral Resolution Sounders in NWP, 28 June–1 July 2004, Reading, UK, pp. 97–112 (2004); available at http://www.ecmwf.int/publications/library/do/references/list/17444.

♦

Long-Range, Low-Frequency, Atmospheric Sound Propagation Physics

D.P. Drob[1] and M.A. Hedlin[2]

[1] *Space Science Division*

[2] *Scripps Institution of Oceanography, University of California*

Introduction: Subaudible low frequency atmospheric sound in the 0.02 to 10 Hz frequency band, also known as infrasound, is continually produced around the globe by a variety of natural and manmade sources. Much like seismic signals, infrasound provides a means to detect, locate, and characterize explosions and other high-energy events. Infrasound can propagate for thousands of kilometers in atmospheric waveguides because the acoustic attenuation at these frequencies is weak. First used to detect approaching aircraft and artillery batteries during World War I, today's infrasound monitoring applications range from the supplementation of civilian natural-hazard warning systems to a component of the International Monitoring System (IMS) of the Comprehensive Nuclear Test Ban Treaty Organization (CTBTO).[1,2]

To accurately detect, locate, and characterize unknown infrasound events of interest over regional and long-range distances, detailed knowledge the atmosphere, often to very high altitudes, is required. One of the challenges of infrasound monitoring is that the atmosphere is constantly changing. Infrasound signal propagation characteristics thus vary widely with geographic location, propagation direction, time-of-day, and day-of-year.[1] Through research in remote sensing, acoustic wave propagation, atmospheric modeling, and other fields, the Naval Research Laboratory (NRL) has developed the means to account for this variability and compute time-dependent infrasound propagation characteristics in near real time. Figure 7 shows a local atmospheric profile from the hybrid Ground to Space (G2S) atmosphere specification technique developed at NRL (left panel) along with the resulting computed infrasound signal propagation characteristics (right panels). Research into the effects of subgrid-scale atmospheric irregularities has also further increased the fidelity of infrasound propagation calculations.

Making Sense of Infrasound Network Observables: The locations and status of the permanent infrasound arrays in the CTBTO's infrasound monitoring network — which complements the IMS seismic and radionuclide ground-based nuclear explosion monitoring networks — are shown in Fig. 8(a). Each IMS infrasound array is comprised of several distributed high-gain pressure sensors spaced approximately 750 m apart. For each infrasound array in the network, automated signal processing algorithms continuously compute the observed line of bearing (incoming signal direction), coherency measures, amplitude, and frequency content of any detected infrasound signals. This information is then combined with the infrasound detections from other infrasound stations via standard seismic network data processing techniques in order to identify potential events of interest. The automated event bulletins generated by the systems are then reviewed by human analysis in conjunction with the data from the other monitoring technologies to identify any potential Comprehensive Nuclear Test Ban Treaty violations. Individual single-element broadband seismic sensors are also capable of detecting the infrasound that propagates through the atmospheric waveguides. Shown in Fig. 8(b) is the National Science Foundation EarthScope Transportable Array seismic network that has provided data for NRL's basic research in infrasound propagation physics.

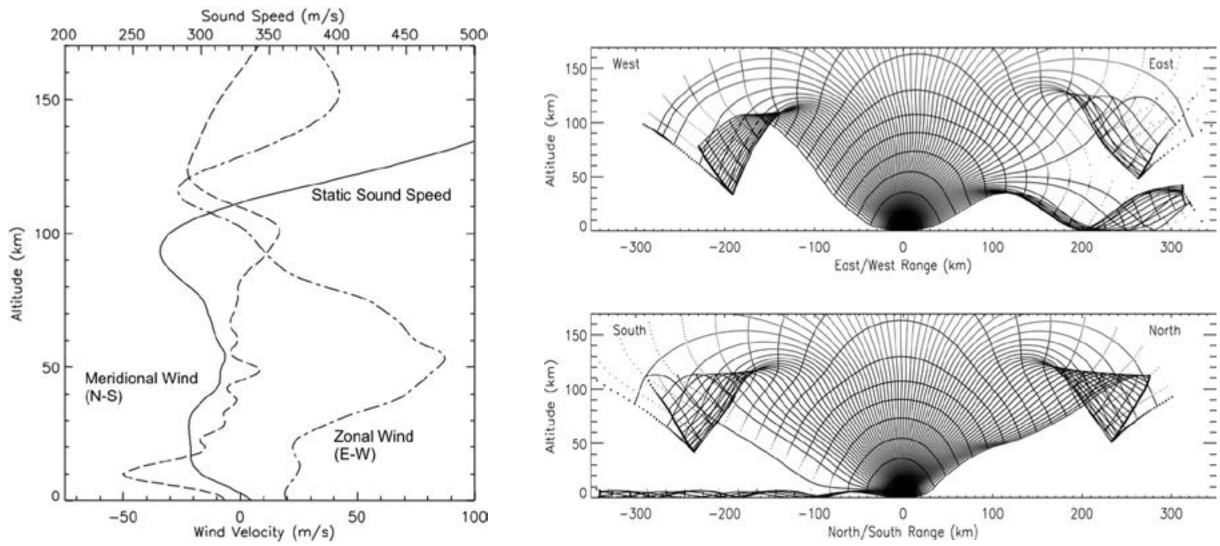

FIGURE 7
Left panel: The atmospheric zonal wind velocity (dash-dotted line), meridional wind velocity (dashed line) and sound speed (solid line) profiles at 45°S, 260°E on June 17, 2001 at 0600 UTC. Right panel: A 1000 s infrasound ray-tracing simulation performed in the east/west (top) and north/south (bottom) planes. The location and evolution of the composite wave front(s) are shown at 5 min intervals.

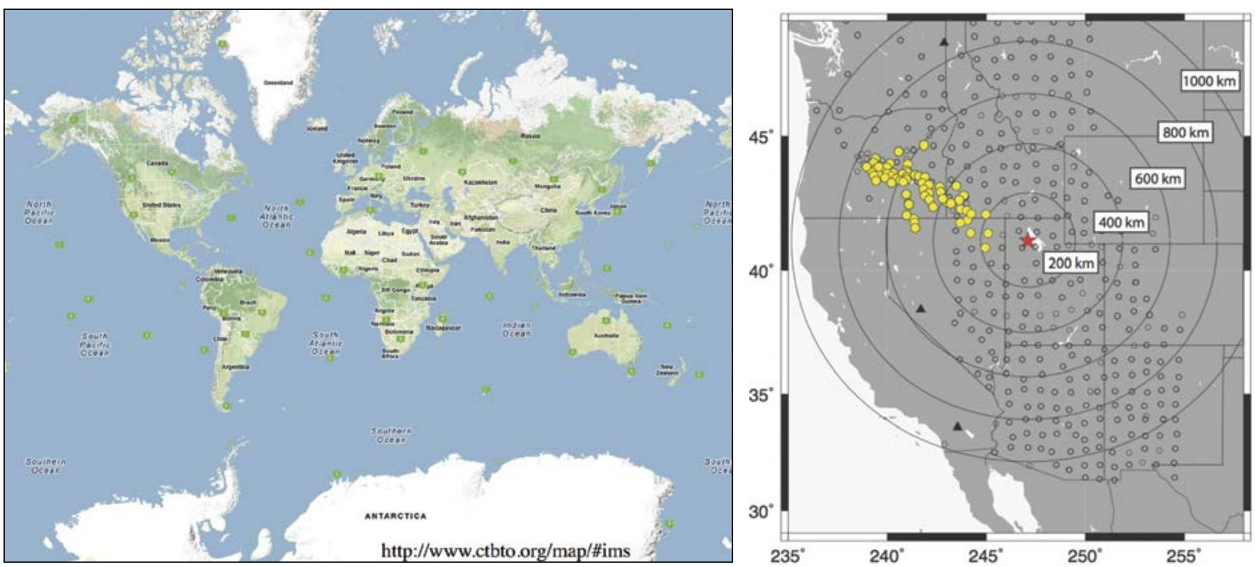

(a) (b)

FIGURE 8
(a) Location of the 60 infrasound stations (green squares) in the Comprehensive Nuclear Test Ban Treaty Organization (CTBTO) International Monitoring System (IMS). (b) The National Science Foundation EarthScope Transportable Array (TA) comprises 400 broadband seismic stations (empty circles) installed on a Cartesian grid spanning 2,000,000 km^2. Through individual station redeployments, the TA network is gradually moving to the east coast. Also shown is the dense, permanent, 73-station, High Lava Plains Broadband Seismic Experiment network (yellow circles). Three permanent infrasound arrays are also shown (black triangles). The location of the Utah Test and Training Range (UTTR) is indicated (red star).

The ground-based infrasound monitoring technologies developed at NRL provide global ground-to-space specification of the atmosphere along with the supporting acoustic propagation codes needed to calculate infrasound propagation characteristics in near real time. These characteristics can then be used in network processing algorithms to lower system false alarm rates, increase network detection thresholds, and reduce source location uncertainties. These gains are achieved by accounting for several factors in near real time: how infrasound signals travel at different velocities in the various waveguides (e.g., upwind versus downwind); to what extent observed back azimuths deviate from the true great circle path back to a source as the result of cross-track wind effects; and how specific atmosphere waveguides might vary with range.

Atmospheric Wave–Wave Interactions: In addition to the need to account for the time-dependent macroscopic behavior of the atmosphere in propagation calculations, the importance of also accounting for unresolved small-scale atmospheric buoyancy fluctuations (known as atmospheric gravity waves) was recently recognized. The presence of these waves explains frequently observed infrasound signals in the classical near-field shadow zones, as well as how quickly infrasound signals lose their coherency over regional distances. Much like turbulence, the atmosphere's internal gravity waves arise from wind flow over mountains, cumulus convection, and large-scale atmospheric instabilities. The intermediate and small-scale part of the internal gravity wave spectrum cannot be deterministically resolved by today's operational meteorological systems. Therefore, just as subgrid-scale turbulence is parameterized in aerodynamic drag calculations, internal gravity wave interactions can be treated in a similar way for infrasound propagation calculations. A stochastic internal gravity wave model suitable for infrasound propagation modeling calculations was developed at NRL in partnership with the Scripps Institution of Oceanography, Raytheon BBN Technologies, and Computational Physics Incorporated.[3] Adapted from the gravity wave parameterizations used within numerical weather prediction and climate general circulation models, the resulting NRL stochastic wave model is fully three-dimensional, time dependent, and physically self-consistent with the observed atmospheric background state.

To validate the updated propagation physics model, it was used to predict waveforms and signal travel times for over 100 seismic stations within the EarthScope seismic network. These stations routinely detected solid rocket body destruction events (typically >15 ton TNT equivalent) that occurred at the Utah Test and Training Range (UTTR) during summer months as part of the STrategic Arms Reduction Treaty (START) protocol. Figure 9 shows the predicted and observed results for a UTTR event on June 16, 2008. Included for comparison (in green) are the classical deterministic ray trace results through the unperturbed G2S atmospheric specifications. The model calculations (red) explain the detection of signals in the classical near-field shadow zone (a.k.a. the classical zone of silence), as well as traditionally anomalous early arrivals at greater distances. The regions of the Transportable Array record section where wave–wave interactions are predicted to fill in classical shadow zones, as well as extend the band heads of secondary acoustic arrivals, are highlighted by the blue ovals. The purple oval highlights the regions where elevated evanescent arrivals (the traditionally anomalous second bounce range early arrivals) are also successfully predicted. The statistical scatter in the ensemble calculations also closely matches the observed waveform signal durations.

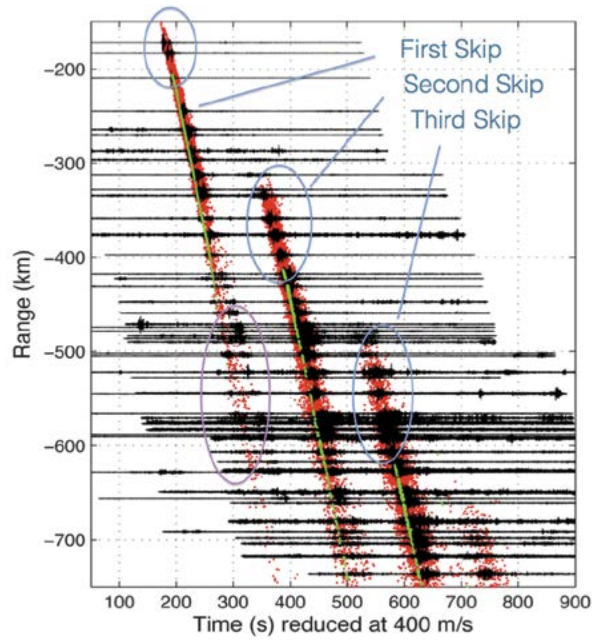

FIGURE 9
A comparison of classical acoustic travel-time predictions (green) and the new NRL stochastic ensemble ray trace predictions (red) against observed infrasound waveforms (black) by the network shown in Fig. 2(b) for a UTTR event on June 16, 2008. The observed waveforms are shifted in time with range by an average group velocity of 400 m/s. The ovals indicate regions of differences between classical ray theory and the observations, which can now be reconciled by accounting for internal atmospheric gravity fluctuations.

Summary: Infrasound research has burgeoned in conjunction with the increased sophistication of available atmospheric specifications and acoustic propagation modeling codes developed by NRL. The fidelity of information such as source location, origin time, and event classification that can be derived on the basis of infrasound network data alone (i.e., without being supplemented with seismic network data or eyewitness accounts) depends to a great extent on the state and knowledge of the atmosphere along the entire acoustic propagation path. As the result of our research, scientific knowledge of how computed range–bearing solutions and other infrasound propagation characteristics are affected by the spatiotemporal variability of the atmosphere has improved measurably. The new knowledge will lead to improvements in infrasound network detection performance metrics, minimum detection thresholds, automatic detection algorithm false alarm rates, and event bulletin source location accuracy.

[Sponsored by ONR, Department of Energy National Nuclear Security Administration, and U.S. Army Space Missile Defense Command]

References

[1] D.P. Drob, M. Garcés, M. Hedlin, and N. Brachet, "The Temporal Morphology of Infrasound Propagation," *Pure Appl. Geophys.* **167**, 437–453 (2010); doi:10.1007/s00024-010-0080-6.

[2] D. Drob, J. Picone, and M. Garcés, "Global Morphology of Infrasound Propagation," *J. Geophys. Res.* **108**, 4680 (2003); doi:10.1029/2002JD003307.

[3] D.P. Drob, D. Broutman, M.A. Hedlin, N.W. Winslow, and R.G. Gibson, "A Method for Specifying Atmospheric Gravity-Wave Fields for Long-Range Infrasound Propagation Calculations," *J. Geophys. Res.*, in press, doi:10.1029/2012JD018077.

♦

Smart Voyage Planning — Saving Fuel by Using Environmental Forecasts to Aid in Ship Routing

J. Cook and J. Hansen
Marine Meteorology Division

Introduction: The Department of Defense (DoD) is responsible for nearly 2% of the petroleum consumption in the United States. The Navy consumes approximately 25% of the DoD portion, roughly 28.5M barrels (bbls) in FY2008, and maritime operations represent about 50% of the Navy total.[1] With energy consumption and costs increasing in a climate of resource conservation, energy independence, and fiscal responsibility, the Chief of Naval Operations (CNO) established Task Force Energy with these objectives: raise visibility and awareness of energy as a strategic resource; optimize energy considerations in budgeting and acquisition; and recommend Navy-wide energy conservation, environmental stewardship, and alternative energy strategies.

In response to the CNO, the Secretary of the Navy developed focused energy goals of sailing the "Great Green Fleet" by 2016 with a demonstration in 2012, and reducing nontactical petroleum use by 50% by 2020.

As part of the Naval Sea Systems Command (NAVSEA) Energy Office program, the NRL Marine Meteorology Division (MMD) worked with Itri Corp. in coordination with DRS Defense Solutions, LLC, to address these energy goals by developing the Smart Voyage Planning Decision Aid (SVPDA). SVPDA is a software application used to optimize ship transit routing for fuel savings. The software incorporates ship hull, mechanical, and electrical (HM&E) models combined with a sophisticated treatment of real-time environmental forecast data to produce route guidance that optimizes fuel efficiency while ensuring ship safety. SVPDA was demonstrated during the Rim of the Pacific 2012 exercise, with fuel efficient route guidance provided from a prototype system at NRL MMD to USS *Princeton* (CG 59) via Fleet Weather Center San Diego (FWC-SD).

Methodology: The Navy has devoted considerable effort to develop the operational global ensemble forecast system consisting of the Navy Operational Global Atmospheric Prediction System (NOGAPS), WAVE WATCH III (WW3), and the global Navy Coastal Ocean Model (NCOM) systems. (NOGAPS was used in development and has since transitioned to NAVGEM – see pages 138 to 140.) Ensembles refer to a collection of numerical model forecast runs from the same start time, with each run (or "member") having a slightly different, but realistic (within the bounds of expected uncertainty) set of initial conditions. The result is a suite of forecasts spanning the range of possible future states. Ensembles have the potential to improve forecasting over deterministic systems (a single forecast run) through improvements in data assimilation and with their additional information about the expected distribution of forecast environmental parameters. Recently, NRL MMD worked with Itri Corp. to develop the Ensemble Forecast Application System (EFAS) to provide a framework to easily utilize ensemble data and perform automated post-processing to improve the forecast statistics. Post-processing refers to the practice of correcting model output based on the historical performance of the forecast system.

EFAS is configurable, not model specific, and produces a consensus based on bias correction (removal of systematic error) over a 30-day period that conveys deterministic-like values (for ease of interfacing with applications expecting deterministic data) and confidence in the consensus within a user-defined tolerance of forecast error. EFAS outputs were interfaced to the Ship Tracking and Routing System (STARS) to provide improved guidance for ship routes as part of SVPDA. Experiments with EFAS showed that a hybrid combination of raw ensemble average and bias-corrected ensemble average provided the optimum set of environmental parameters for STARS. These parameters are shown in red in Table 1.

During RIMPAC 2012, NRL MMD, Itri Corp., and DRS worked with FWC-SD and USS *Princeton* and USS *Chafee* (DDG 90) to demonstrate SVPDA. FWC-SD watch standers initiated route requests after entering the ship's Movement Report (MOVEREP) information into the operational Joint METOC Viewer (JMV) software. JMV produced a SVPDA request, which was e-mailed to NRL MMD for servicing. NRL MMD used

Table 1 — Environmental Data Products from EFAS

Parameter	Post-Processed Data from EFAS			
10 meter – U west wind component	16 member NOGAPS forecast	Raw Ensemble Average	Bias Corrected Ensemble Average	Wind Speed Confidence
10 meter – V south wind component	16 member NOGAPS forecast	Raw Ensemble Average	Bias Corrected Ensemble Average	
Sea height (wind wave)	16 member WW3 forecast	Raw Ensemble Average	Bias Corrected Ensemble Average	Sea Height Confidence
Sea period (wind wave)	16 member WW3 forecast	Raw Ensemble Average	Bias Corrected Ensemble Average	
Sea direction (wind wave)	16 member WW3 forecast	Raw Ensemble Average	Bias Corrected Ensemble Average	
Swell height	16 member WW3 forecast	Raw Ensemble Average	Bias Corrected Ensemble Average	
Swell period	16 member WW3 forecast	Raw Ensemble Average	Bias Corrected Ensemble Average	
Swell direction	16 member WW3 forecast	Raw Ensemble Average	Bias Corrected Ensemble Average	
Surface currents – U east component	*NCOM deterministic forecasts used (ensembles were not available)*			
Surface currents – V north component	*NCOM deterministic forecasts used (ensembles were not available)*			

the EFAS output and JMV ship request file to execute a version of STARS modified by DRS to incorporate the ship HM&E models. The STARS output routes were then plotted using Google Earth Geospatial Information Services (GIS) software for quality control and e-mailed back to FWC-SD for consideration by the Ship Routing Officer for forwarding to the ship. Aboard ship, the route recommendations were entered into the Electronic Chart Display and Information System – Navy (ECDIS-N) for navigation and display. Figure 10 shows the sequence of events and data flow.

Engineering, navigation, and environmental logs taken by USS *Princeton* throughout the voyage from Pearl Harbor to San Diego are being used to assess the SVPDA fuel savings effectiveness for the AEGIS Cruisers. Data for assessment will also be collected from additional surface Navy and Military Sealift Command ships that will be issued SVPDA routes in the future. The recorded environment will be compared to the "perfect forecast" created from the retroactively determined best estimate of the environmental conditions along the voyage and to the ensemble weather forecast valid at that time that was used for the recommended SVPDA route. The impact of any variations between the observed values and those used for the recommended route will be assessed. Engineering plant settings and ship speed throughout the voyage will be reconciled. The following will be addressed:

- Fuel savings projections versus measured;
- The fuel burned for the route followed will be compared to the predicted fuel consumed for the SVPDA-recommended route and for the minimum-distance great circle route (with the same start and destination and the same arrival time);
- Ship HM&E model calibration; and
- Individual leg fuel consumptions down to the component level will be compared for the route USS *Princeton* followed and an equivalent SVPDA route generated using the actual route that USS *Princeton* followed and the observed weather during its voyage to determine the validity of the ship HM&E model and identify possible improvements.

As shown in Fig. 11, ship fuel consumption rate increases rapidly with ship speed, approximately 1% to 4% per knot at moderate speeds and about 9% per knot at high speeds. Thus, optimizing the ship speed profile during transit can yield significant fuel savings. Figure 12 shows the impact of the environment, with ship fuel consumption increasing significantly with moderate waves, wind, and currents. At constant speed, fuel consumption in sea state 4 increases by approximately 10% over the calm water value. According to modeling estimates, using SVPDA-optimized transit routing — optimizing the ship route together with the speed profile to avoid adverse environmental conditions — can save approximately 4% in annual fuel costs.

Figure 13 shows an example SVPDA route recommendation for a ship traveling from Guam to Sydney

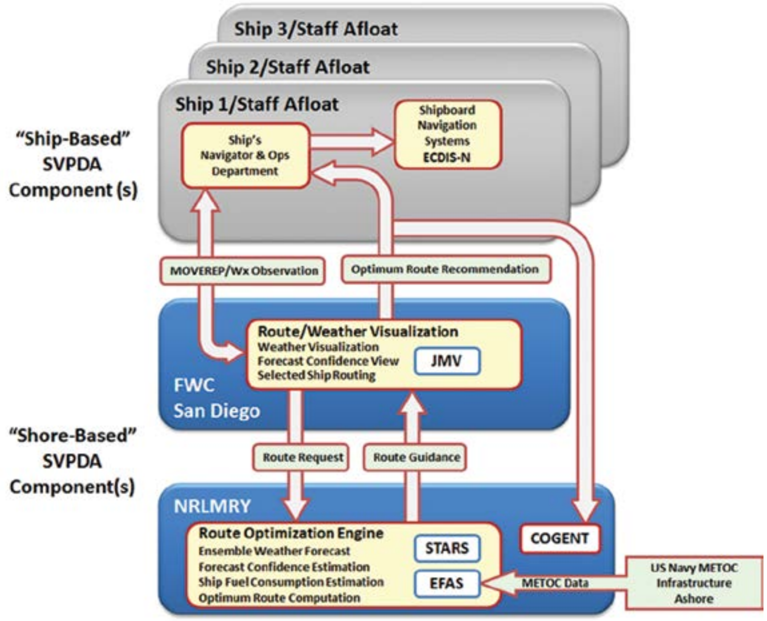

FIGURE 10
Notional components of SVPDA exercised during RIMPAC 2012 showing shore-based EFAS and STARS components at NRL MMD in Monterey and FWC-SD and shipboard components on USS *Princeton* and USS *Chafee*. The COGENT component was not exercised.

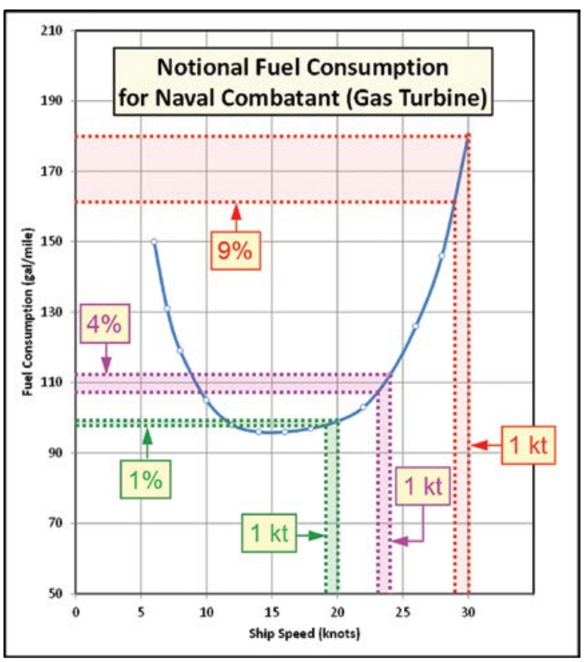

FIGURE 11
Fuel consumption sensitivity to ship speed in calm water.

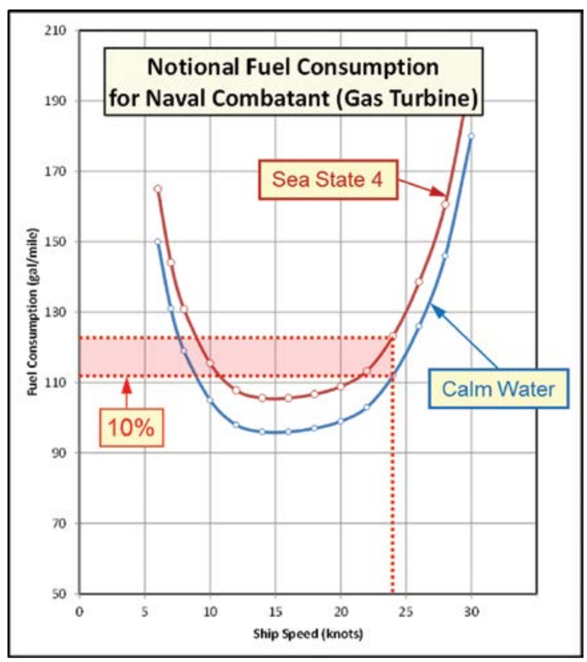

FIGURE 12
Fuel consumption sensitivity to environment with calm water vs sea state 4.

(red line). The great circle route (green line) serves as a baseline for fuel usage comparison. SVPDA selected the route with the minimum overall cost (in gallons of fuel expended) that arrives on time while not exceeding weather-related ship safety limits. The SVPDA route exploits information in the forecasts of adverse weather and the ship's most efficient speed to save 4.5% of fuel expended (savings over 16,500 gal) in spite of a longer distance traveled (3029 nmi vs 3595 nmi); the arrival times are the same.

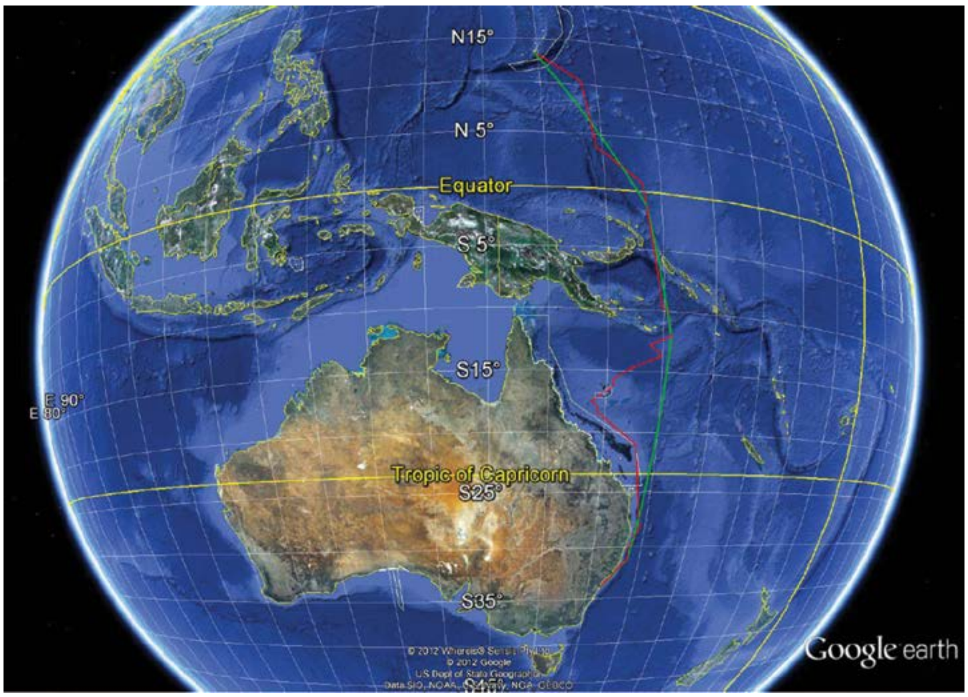

FIGURE 13
SVPDA-recommended minimum fuel route (red line) compared to great circle route baseline (green line) from Guam to Sydney.

Conclusions: SVPDA is a technology that blends a unique, sophisticated treatment of environmental ensemble forecast data with ship HM&E models to provide ship transit recommendations optimized for fuel efficiency and ship safety. SVPDA may be used ashore for ship scheduling with a focus on minimizing fuel usage and it may be enhanced to include environmental mission impact parameters to help improve mission effectiveness and to maximize ship hull life expectancy.

[Sponsored by NAVSEA]

Reference
[1] RADM P. Cullom, Navy Task Force Energy Briefing, Director of Fleet Readiness, OPNAV N43 (2010).

♦